Effect of an in-plane magnetic field on the electronic states and intraband transitions in quasi-periodic Fibonacci superlattices

1995 J. Phys.: Condens. Matter 7 9799

(http://iopscience.iop.org/0953-8984/7/50/014)

J. Phys.: Condens. Matter 7 (1995) 9799–9810. Printed in the UK

Effect of an in-plane magnetic field on the electronic states and intraband transitions in quasi-periodic Fibonacci superlattices

M de Dios-Leyva†, A Bruno-Alfonso†, E Reyes-Gomez† and Luiz E Oliveira‡

† Department of Theoretical Physics, University of Havana, San Lazaro y L, Vedado 10400, La Habana, Cuba

‡ Instituto de Física, Universidade Estadual de Campinas - Unicamp, Caixa Postal 6165, Campinas, São Paulo, 13083-970, Brazil

Received 25 May 1995

Abstract. Quasi-periodic GaAs–(Ga, Al)As Fibonacci superlattices under in-plane magnetic fields are studied within the effective-mass approximation. Electron-envelope wavefunctions, magnetic subbands and intraband transition strengths are obtained using a parabolic model for the conduction band, and via an expansion in harmonic-oscillator wavefunctions. Calculations are performed for magnetic fields related by integer powers of the golden mean $\tau = (1+5^{1/2})/2$. It is shown that, for magnetic field values scaled by τ^{2n}, the corresponding magnetic levels, electron wavefunctions and transition strengths essentially exhibit a self-similar or anti-self-similar behaviour as appropriate for a GaAs–(Ga, Al)As Fibonacci superlattice. Also, for a given magnetic field, the intraband transition strengths have similar properties to those found for the case of periodic superlattices. The intraband absorption coefficients are calculated for magnetic field values scaled by τ^{2n}, and theoretical absorption spectra, when properly scaled, are shown to be self-similar (for even n) or anti-self-similar (for odd n), a result which could be experimentally verified in n-doped GaAs-(Ga, Al)As Fibonacci superlattices.

1. Introduction

Since the pioneering work of Esaki and Tsu [1], modern growth techniques such as molecular-beam epitaxy (MBE) and metal–organic chemical vapour deposition have made possible the realization of high-quality semiconducting heterostructure systems consisting of alternating layers of two different semiconductors with controlled layer thicknesses and sharp interfaces between the layers. Because of the potential device applications of such systems, much work [2] has been devoted to understanding the unique nature of the electronic states associated with semiconducting superlattices (SLs) and heterostructures.

In recent years, there has been considerable interest in understanding the physical properties of quasi-periodic SLs [3, 4] because such a system represents an accessible and intermediate case between periodic and disordered solids. The first realization of such a quasi-periodic SL was reported by Merlin *et al* [5] and consisted of MBE-grown alternating layers of GaAs and AlAs forming a Fibonacci sequence in which the ratio of incommensurate periods was approximately equal to the golden mean $\tau = (1+5^{1/2})/2$. Photoluminescence excitation spectroscopy experiments on GaAs–(Ga, Al)As Fibonacci superlattices (FSLs) were performed by Laruelle and Etienne [6]. A theoretical study of the effects of a magnetic

0953-8984/95/509799+12$19.50

field parallel to the layers in a GaAs–(Ga, Al)As FSL was made by Wang and Maan [7], whereas electric field effects in FSLs were investigated by Laruelle *et al* [8]. Recently, Munzar *et al* [9] have shown that the electronic structure of FSLs exhibits multifractal properties, which manifest themselves also in the experimental reflectance spectra.

The existence of Landau levels in a GaAs–(Ga, Al)As FSL with magnetic fields applied parallel to the layers was clearly observed by Maan and co-workers [10]. Moreover, they measured the magneto-optical spectra of this system and suggested that the spectra exhibit self-similarity at field values scaled by τ^2. This experimental result has led us to investigate theoretically the magnetic levels, electron wavefunctions, transition strengths [11, 12] and intraband absorption coefficients of GaAs–(Ga, Al)As quasiperiodic FSLs under in-plane magnetic fields.

In section 2, we describe the type of GaAs–$Ga_{1-x}Al_xAs$ FSL considered in the calculation. The effective Hamiltonian, the electron wavefunctions, the transition matrix elements and the intraband absorption coefficients are discussed in section 3. The results and discussion are in section 4. Finally, in section 5 we present our conclusions.

2. Quasi-periodic Fibonacci superlattices

In this work we focus our attention on the GaAs–$Ga_{1-x}Al_xAs$ FSL studied by Maan and co-workers [7, 10]. This system was MBE-grown and consists of a Fibonacci alternating sequency of layers of $Ga_{1-x}Al_xAs$ (elementary block a) and GaAs (elementary block b). The generation w_n is obtained with the concatenation of $w_{n-2}(w_{n-1})$ and $w_{n-1}(w_{n-2})$ if n is odd (even), with $w_1 = a$ and $w_2 = b$. One can then see that the number of F_n elementary blocks in w_n follows the Fibonacci sequence $F_n = F_{n-1} + F_{n-2}$, with $F_1 = F_2 = 1$. The ratio F_n/F_{n-1} converges towards the golden mean τ for increasing n, and the numbers of elementary blocks a and b in w_n are F_{n-2} and F_{n-1}, respectively. One of the most important consequences of the generation procedure considered above is the self-similarity of the resulting structure: the transformations (ab → a, abb → b) and (b → a, ab → b) transfer w_n into w_{n-2} and w_n into the reverse of w_{n-1}, respectively [7, 10] (figure 1). Furthermore, by removing the first and last elementary blocks of a given generation w_n, one obtains a modified generation w'_n which contains an inversion centre [13], corresponding to points O in figure 1. Therefore, for a sufficiently large value of n, this property would correspond to symmetrical behaviour of, for instance, the energy spectra (as functions of the orbit-centre position) and wavefunctions (as functions of the z coordinate along the growth direction and for orbit centres at the inversion point) of the GaAs–(Ga, Al)As FSL, if boundary effects are neglected.

For a FSL in the $B_\parallel$ configuration (in-plane magnetic field), the electrons orbit in a plane perpendicular to the layers with an orbit radius $l_B = (\hbar c/eB)^{1/2}$. Therefore, the effective potential seen by the electrons depends on the magnetic field B, and l_B is obviously a characteristic length scale in the study of such systems. Wang and Maan [7] showed, by using perturbation theory, that scaling of τ^{2n} in the magnetic field and therefore of $1/\tau^n$ in the length (orbit radius), with integer n, leads to either self-similarity or 'anti-self-similarity' in the energy-level structure, and to self-similarity in the density of states (see the appendix for an alternative demonstration). It is not difficult to show [7] that the transformations (ab → a, abb → b) and (b → a, ab → b) correspond to scaling with $n = 2$ and $n = 1$, respectively. As a result, the relation $d_b/d_a = \tau$ is a necessary condition [7] to study similarity properties in a FSL in the $B_\parallel$ configuration, where d_b and d_a are the thicknesses of well and barrier layers, respectively. In what follows, we limit ourselves to the cases of scaling of τ^{2n} in the magnetic field, with $n = 1$ and 2.

3. Effective Hamiltonian, electron wavefunctions, transition matrix elements and intraband absorption coefficients

We define y as the growth axis of the GaAs–$Ga_{1-x}Al_xAs$ FSL and consider an in-plane magnetic field applied along the z direction. Then, if we choose the gauge $A = (-yB, 0, 0)$, the Hamiltonian for the electron in the conduction band, within the effective-mass approximation and with a parabolic model for the conduction band, is given by

$$H = [p + eA/c]^2/2m_c + V(y) \tag{1}$$

where $-e$ is the electron charge, m_c is the conduction-band effective mass, $p = -i\hbar\nabla$, and $V(y)$ is the FSL potential, equal to zero in the wells and to V_0 in the barriers. The origin of energy is taken at the bottom of the bulk-GaAs conduction band.

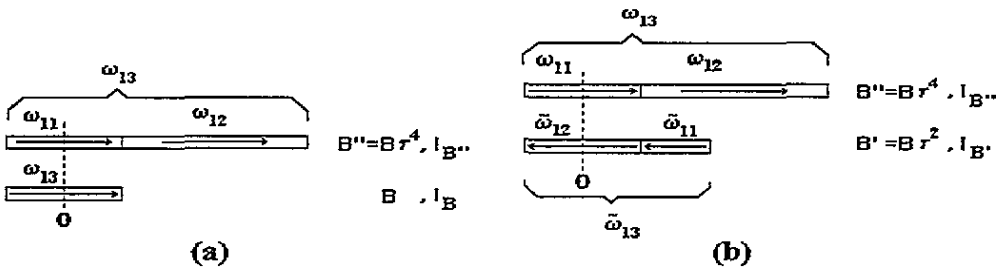

Figure 1. (a) Schematic view of the Fibonacci generations $w_{13} = w_{11}w_{12}$ (in units of the cyclotron radius $l_{B''}$) and w_{13} (in units of l_B). (b) Schematic view of generations $w_{13} = w_{11}w_{12}$ (in units of $l_{B''}$) and the reverse of w_{13}, i.e. $\tilde{w}_{13} = \tilde{w}_{12}\tilde{w}_{11}$ (in units of $l_{B'}$). The magnetic fields are B, $B' = B\tau^2$ and $B'' = B\tau^4$.

If one uses the translational symmetry in the x and z directions, the eigenfunctions of (1) may be chosen as

$$|n, k_\perp\rangle = \frac{\exp(ixk_x)}{(L_x)^{1/2}} \frac{\exp(izk_z)}{(L_z)^{1/2}} \phi_{nk_x}(y) \tag{2}$$

where $k_\perp = (k_x, k_z)$, $n = 0, 1, 2, \ldots$, indicates the Landau-subband index, and L_x and L_z are the linear dimensions of the sample in the x and z directions, respectively. The eigenfunctions (2), which we assume to be orthonormalized, describe states with well defined values of k_z, the energy $E_n(k_z, y_0) = \epsilon_n(y_0) + \hbar^2k_z^2/2m_c$, and the orbit centre position $y_0 = k_x l_B^2$.

In the study of the optical transition matrix elements in a FSL in the $B_\parallel$ configuration, we limit ourselves to the case of intraband transitions between electronic magnetic levels (magnetic subbands associated with the conduction band). A similar study was reported recently by de Dios-Leyva *et al* [11, 12] for the case of periodic GaAs–(Ga, Al)As SLs. As in the usual experimental situation, our calculations will be performed in the $B_\parallel$ configuration with light propagation perpendicular to the magnetic field (Voigt geometry). In this case, the polarization vector ϵ of the radiation is parallel to the layers and may be taken perpendicular to the magnetic field, i.e. parallel to the x axis. Note that optical transitions with ϵ parallel to B cannot be excited [11]. Under these conditions, the matrix element between an initial state $|n, k_\perp\rangle$ and a final state $|n', k'_\perp\rangle$, in the dipole approximation, is given by [11]

$$M_{n'n}(k'_\perp, k_\perp) = C\langle n', k'_\perp | p_x + eA_x/c | n, k_\perp\rangle \tag{3}$$

where C is a pre-factor which contains the amplitude of the photon vector potential. Using the wavefunctions of equation (2) it is straightforward to show that

$$M_{n'n}(k'_\perp, k_\perp) = \delta_{k'_\perp, k_\perp} N_{n'n}(y_0) \tag{4}$$

with

$$N_{n'n}(y_0) = \frac{\sqrt{2}}{l_B}\langle \phi_{n'y_0} | y - y_0 | \phi_{ny_0} \rangle. \tag{5}$$

The matrix elements in (5) are normalized to the matrix element between the ground and first-excited Landau levels in the bulk (i.e. $V(y) = 0$ in equation (1)). From (4), it is obvious that only vertical transitions may occur and in what follows we assume that $k'_\perp = k_\perp$. In the theoretical study of the intraband optical absorption in FSLs in the $B_\parallel$ configuration and Voigt geometry, it is convenient to consider explicitly the transition strengths [12], which may be defined as

$$T_{n,n'}(y_0) = |N_{n'n}(y_0)|^2 \tag{6}$$

and satisfy the following sum rule [12]:

$$\sum_{n'=0} \frac{\epsilon_{n'}(y_0) - \epsilon_n(y_0)}{\hbar\omega_c} T_{n,n'}(y_0) = 1 \tag{7}$$

where $\omega_c = eB/cm_c$ is the cyclotron frequency. From the above equations, it is straightforward to evaluate the intraband absorption coefficient $\alpha(\omega)$ for n-doped GaAs–(Ga, Al)As FSLs, as discussed in a previous work by one of the present authors and a co-worker [12].

Let us now consider the Schrödinger equation for the functions $\phi_{nk_x}(y)$ introduced in equation (2). When all energies and lengths, for a given magnetic field B, are expressed in reduced units of the cyclotron energy $\hbar\omega_c$ and magnetic length l_B, respectively, this equation takes the form

$$\left(-\tfrac{1}{2}\frac{d^2}{du^2} + \tfrac{1}{2}(u - u_0)^2 + v(u)\right)\Psi(u - u_0) = E(u_0)\Psi(u - u_0) \tag{8}$$

where $y = ul_B$, $y_0 = u_0 l_B$, $v(u) = V(y)/\hbar\omega_c$, $E(u_0) = \epsilon_n(y_0)/\hbar\omega_c$ and $\Psi(u - u_0) = \phi_{nk_x}(y)$.

Of course, in the absence of $v(u)$, the eigenvalues and eigenfunctions of equations (8) are, respectively, $E(u_0) = E_n(u_0) = n + \frac{1}{2}$ and the harmonic-oscillator wavefunctions

$$h_n(u - u_0) = A_n \exp[-(u - u_0)^2/2] H_n(u - u_0) \tag{9}$$

where $n = 0, 1, 2, \ldots$, A_n is a normalization constant, and H_n the Hermite polynomial of order n. In the presence of the $v(u)$ FSL potential, the solutions of equation (8) may be expanded in terms of the set of functions (9), i.e.

$$\Psi(u - u_0) = \sum_{n=0} a_n h_n(u - u_0) \tag{10}$$

where the expansion coefficients a_n satisfy the following system of homogeneous linear equations:

$$\sum_{n=0}[(n + \tfrac{1}{2}) - E(u_0)]\delta_{mn} a_n + \sum_{n=0} v_{mn}(u_0) a_n = 0 \tag{11}$$

with

$$v_{mn}(u_0) = \langle h_m(u - u_0) | v(u) | h_n(u - u_0) \rangle. \tag{12}$$

As will be seen below, a quantity of special interest in the study of the electron wavefunctions and transition strengths is the deviation $\Delta\Psi_n$ of order n, which may be defined as

$$\Delta\Psi_n(u-u_0) = \Psi_n(u-u_0) - h_n(u-u_0) \tag{13}$$

where $\Psi_n(u-u_0)$ is the eigenfunction of equation (8) corresponding to the Landau subband index n, $h_n(u-u_0)$ is the nth harmonic-oscillator wavefunction, u_0 is a specific value of the orbit centre position, and the phase of $\Psi_n(u-u_0)$ is chosen such that $\Delta\Psi_n(u-u_0)$ goes to zero as the FSL potential tends to zero. It is obvious that the set of functions (13) may be used to describe the effect of the FSL potential on the electron wavefunctions.

Equations (10)–(13) will be used to study the properties of the magnetic subbands, electron wavefunctions and intraband transition strengths in GaAs–$Ga_{1-x}Al_xAs$ FSLs in the $B_\parallel$ configuration and Voigt geometry.

4. Results and discussion

As commented above, we focus our attention on the GaAs–$Ga_{1-x}Al_xAs$ FSL considered by Maan and co-workers [7, 10]. The 60–40% rule for the band offset is used in the calculations, with the total band-gap difference ΔE_g, between GaAs and $Ga_{1-x}Al_xAs$, given as a function of the Al concentration x by ΔE_g (eV) $= 1.247x$. The values of the conduction-band effective mass m_c, Al concentration, well width d_b and barrier width d_a were chosen as $m_c/m_0 = 0.067$, $x = 0.2$, $d_b = 1.69$ nm and $d_a = 1.12$ nm. Note that, with this choice for d_a and d_b, one has [7] $d_b/d_a \simeq \tau$, and anti-self-similarity or self-similarity in the length scale for two different magnetic fields related by τ^2 or τ^4, respectively, is guaranteed. Also, in order to satisfy this relation, the following magnetic field values [7] were used in the calculations: $B = 2.92$ T, $B' = B\tau^2 = 7.64$ T and $B'' = B\tau^4 = 20$ T. The corresponding magnetic lengths are related by $l_B = \tau l_{B'} = \tau^2 l_{B''}$, and the transformations (ab $\rightarrow$ a, abb $\rightarrow$ b) and (b $\rightarrow$ a, ab $\rightarrow$ b) considered above correspond to scaling of τ^2 and τ in the length [7], respectively (see figure 1).

The ten lowest magnetic subbands for $B = 2.92$ T, $B' = B\tau^2 = 7.64$ T, and $B'' = B\tau^4 = 20$ T are shown in figure 2 as functions of the orbit centre position and for zero wavevector in the direction of the magnetic field. In figures 2(a) and 2(b) we have also drawn, in the lower part, a section of the GaAs–$Ga_{0.8}Al_{0.2}As$ FSL potential in reduced units (whenever the field is scaled by τ^{2n}, the FSL potential in reduced units is, of course, scaled by $1/\tau^{2n}$). Note that the origin of coordinates was taken at the inversion centres of the w_{13} Fibonacci generation for $B = 2.92$ T, of the $\tilde{w}_{12}$ generation for $B' = B\tau^2 = 7.64$ T, and of the w_{11} generation for $B'' = B\tau^4 = 20$ T (cf figures 1 and 2). As commented before, the symmetrical behaviour of the energy spectra with respect to the inversion centre is apparent in figure 2. Also, as one can see, scaling of τ^4 and τ^2 in the field leads to self-similarity (see figure 2(a)) and anti-self-similarity (cf figure 2(b)) of the energy-level structure, as expected for a GaAs–(Ga, Al)As FSL. In displaying the magnetic subbands for these values of the magnetic field, the $B\tau^4$ (20 T) magnetic subbands (in reduced units) were rigidly shifted upwards in order that firstly in figure 2(a) the $n = 0$ subbands would essentially coincide (the shift in the case of the $B\tau^4$ (20 T) magnetic subbands is given by $\beta = V_0/\tau^3$ upwards, as shown in the appendix), and secondly in figure 2(b) the average energies (in reduced units) of the $n = 0$ subbands would coincide. Calculations were done with varying sets of basis functions, and convergence was achieved with 500, 400 and 300 harmonic-oscillator wavefunctions in the basis set for B, $B\tau^2$ and $B\tau^4$, respectively. Our results for the magnetic-level structure are in good agreement with the calculations of Wang

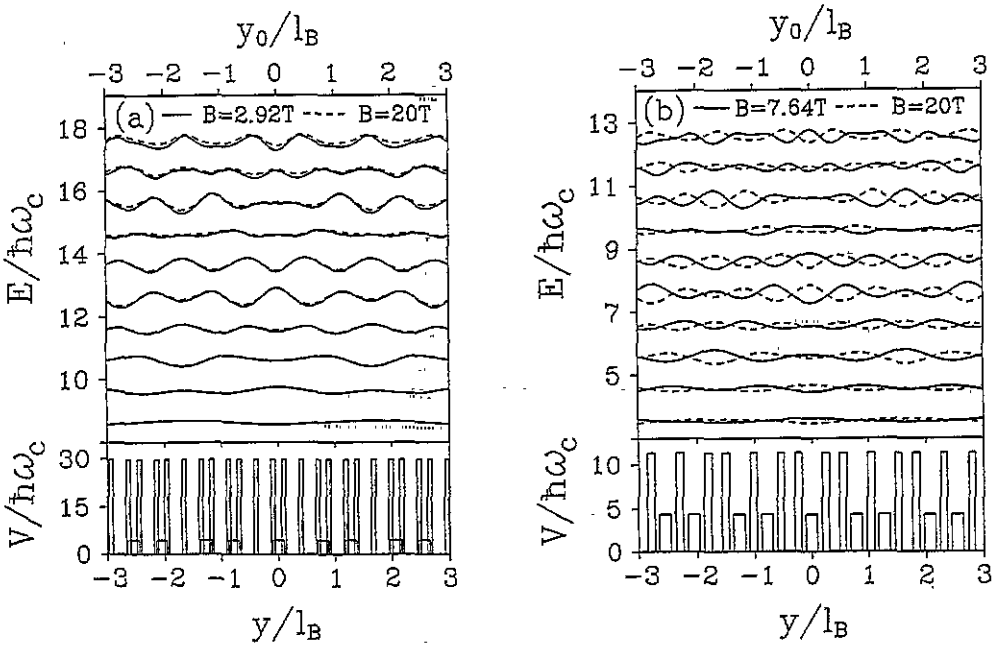

Figure 2. (a) Magnetic subbands of a GaAs–(Ga, Al)As quasi-periodic FSL under an in-plane $B = 2.92$ T (——) and $B'' = B\tau^4 = 20$ T (– – –) as functions of the orbit-centre position, for zero k_z wavevector in the direction of the magnetic field. In the lower part, a section of the Fibonacci potential (at the same fields and around the inversion centre) used in the calculation. Energies and lengths are in units of the cyclotron energy and cyclotron radius, respectively. (b) As in (a), but for $B' = B\tau^2 = 7.64$ T and $B'' = B\tau^4 = 20$ T.

and Maan [7], who computed the magnetic subbands by a finite-element method (note that they used $V_0 = 0.20$ eV, whereas we have used $V_0 = 0.15$ eV which is appropriate for an $x = 0.2$ proportion [10] of Al in the barriers).

Let us now discuss, for the same magnetic fields, some of the properties of the electron wavefunctions. For simplicity, we consider only the wavefunctions corresponding to the ground and first excited states for the y_0 orbit centre at the inversion point, i.e. $y_0/l_B = 0$ (figure 3). One can see that the corresponding wavefunctions at $B = 2.92$ T and $B'' = B\tau^4 = 20$ T (see figures 3(a) and 3(b)) are essentially the same if a very small difference between them is disregarded. This difference in wavefunctions is associated with the fact that the scaled FSL potentials seen by the electrons in different magnetic fields are not the same, and so wavefunctions are overall self-similar (see appendix) but with details (maxima and minima) of the electron wavefunctions clearly associated with the corresponding FSL potential for each magnetic field. For $B' = B\tau^2 = 7.64$ T and $B'' = B\tau^4 = 20$ T, the wavefunctions (see figures 3(c) or 3(d)) are clearly different and at first sight it may appear that their properties are not related. This is not so, however. In order to see the relation, we show in figure 4(a) the deviations $\Delta\Psi_n(u)$ as functions of the position u along the FSL growth direction. For $B' = B\tau^2 = 7.64$ T, these quantities are seen to be essentially anti-self-similar with respect to those of $B'' = B\tau^4 = 20$ T. The anti-self-similarity in $\Delta\Psi$ is quite important in the understanding of the transition-strength structure for magnetic fields related by τ^2. Moreover, in order to illustrate better the details of the electron wavefunctions at $B = 2.92$ T and $B'' = B\tau^4$, we show in figure 4(b) the corresponding deviations $\Delta\Psi_n(u)$. Then, it follows from figures 3(a) and 4(b) that both

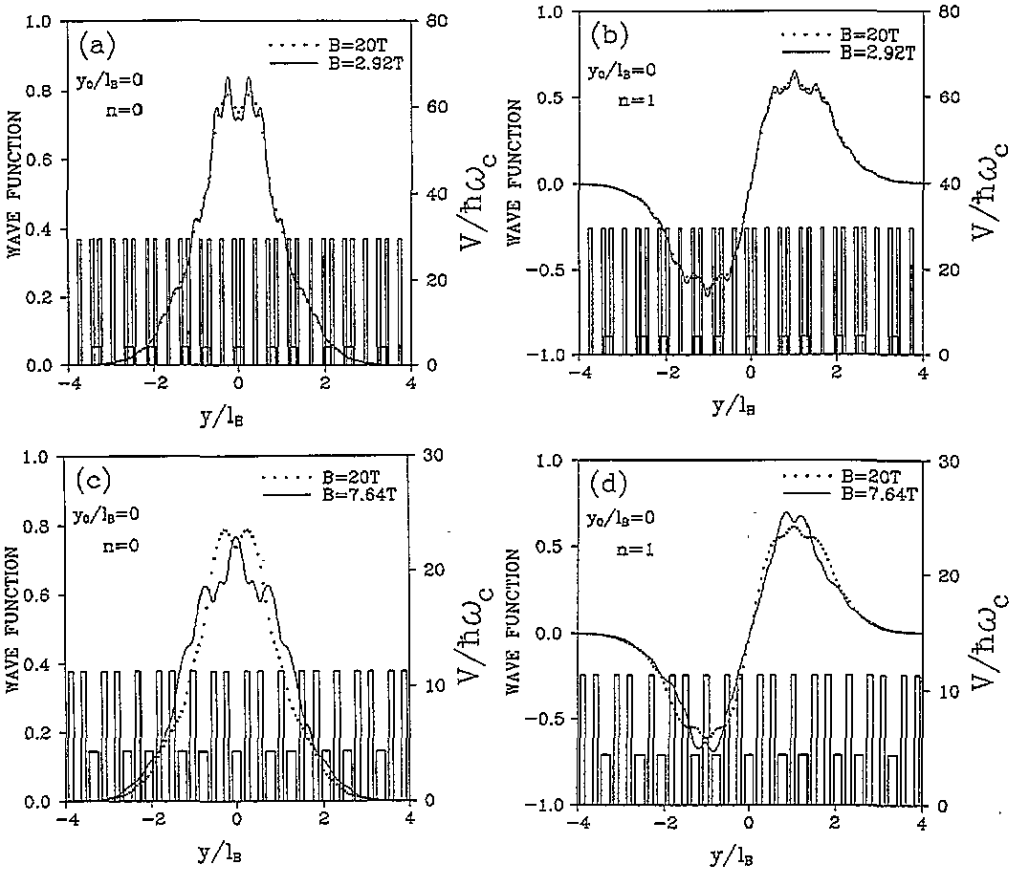

Figure 3. Electron wavefunctions of a GaAs–(Ga, Al)As FSL corresponding to (a) the ground and (b) first excited states for the u_0 orbit centre at the inversion point, and for in-plane magnetic fields $B = 2.92$ T (——) and $B'' = B\tau^4 = 20$ T (·····), as functions of the position along the superlattice growth axis. Also shown is a section of the scaled Fibonacci potentials (at the same fields) used in the calculations; (c) and (d). As in (a) and (b), but for $B' = B\tau^2 = 7.64$ T (——) and $B'' = B\tau^4 = 20$ T (·····).

the electron wavefunctions and the deviations have an approximate self-similar structure for a scaling of τ^4 in the magnetic field. Also, it was found in our numerical calculations that all the above conclusions are valid for the calculated remaining states and orbit centre positions shown in figure 3. Note also that wavefunctions in figure 3 (for the orbit centre at the inversion point) are even or odd with respect to the inversion centre, as commented before.

Taking into account equations (5) and (6) and the self-similarity of the wavefunctions for $B = 2.92$ T and $B'' = B\tau^4 = 20$ T, it is obvious that the corresponding intraband transition strengths $T_{n,n'}$ must also display a self-similar structure as functions of the orbit centre position. This is illustrated in figure 5 which shows some $n \rightarrow n'$ transition strengths for these fields. Note again the symmetric behaviour of the transition strengths with respect to the inversion centre, which implies that transitions involving magnetic Landau levels with $\Delta n =$ even, and for the y_0 orbit centre at the inversion point, are forbidden.

At $B' = B\tau^2 = 7.64$ T and $B'' = B\tau^4 = 20$ T, the properties of the transition strengths (figure 6) are clearly different from those established above for $B = 2.92$ T and

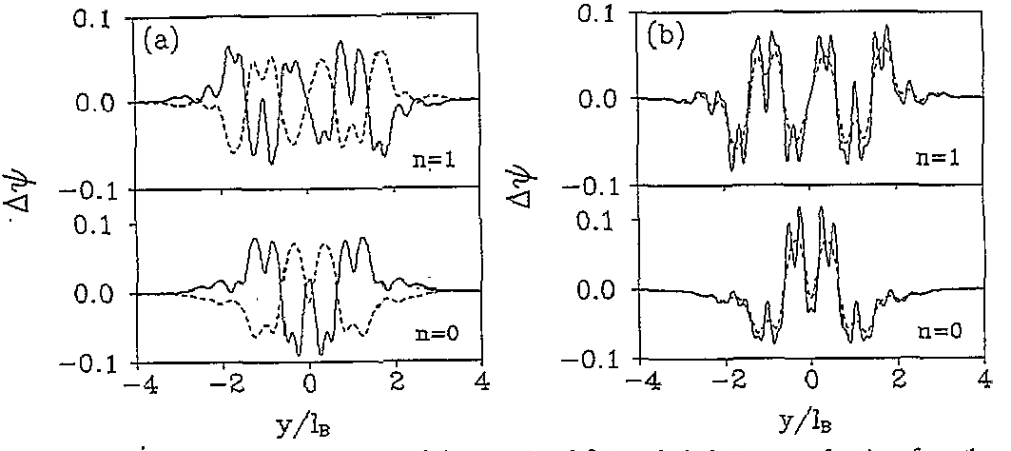

Figure 4. (a) Deviations of the ground and first excited electron wavefunctions from the corresponding harmonic-oscillator wavefunctions for the u_0 orbit centre at the inversion point, and in-plane magnetic fields $B' = B\tau^2 = 7.64$ T (——) and $B'' = B\tau^4 = 20$ T (– – –), as functions of the position along the superlattice growth direction. (b) As in (a), but for $B = 2.92$ T (——) and $B'' = B\tau^4 = 20$ T (– – –).

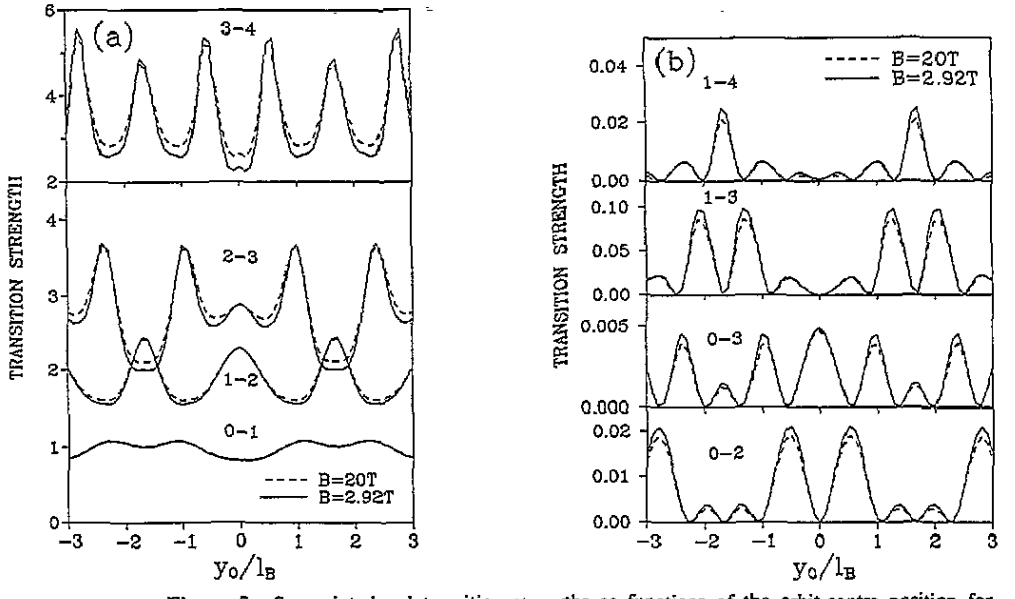

Figure 5. Some intraband transition strengths as functions of the orbit-centre position for $B = 2.92$ T (——) and $B'' = B\tau^4 = 20$ T (– – –): (a) $n \to n+1$ transitions up to $n = 3$; (b) $0 \to 2$, $0 \to 3$, $1 \to 3$ and $1 \to 4$ transitions.

$B'' = B\tau^4 = 20$ T (see figure 5). In fact, whereas the $n \to n+1$ transition strengths display an anti-self-similar behaviour (see figure 6(a)), the $n \to n+k$ transition strengths, with $k \geqslant 2$, essentially exhibit a self-similar structure (cf figure 6(b)). These results follow immediately from the anti-self-similarity of the corresponding deviations $\Delta_n\Psi(\chi)$, which occurs provided that one neglects $|\Delta\Psi_n(\chi)|^2$ (which are relatively small) with respect to $\Delta\Psi_n(\chi)$.

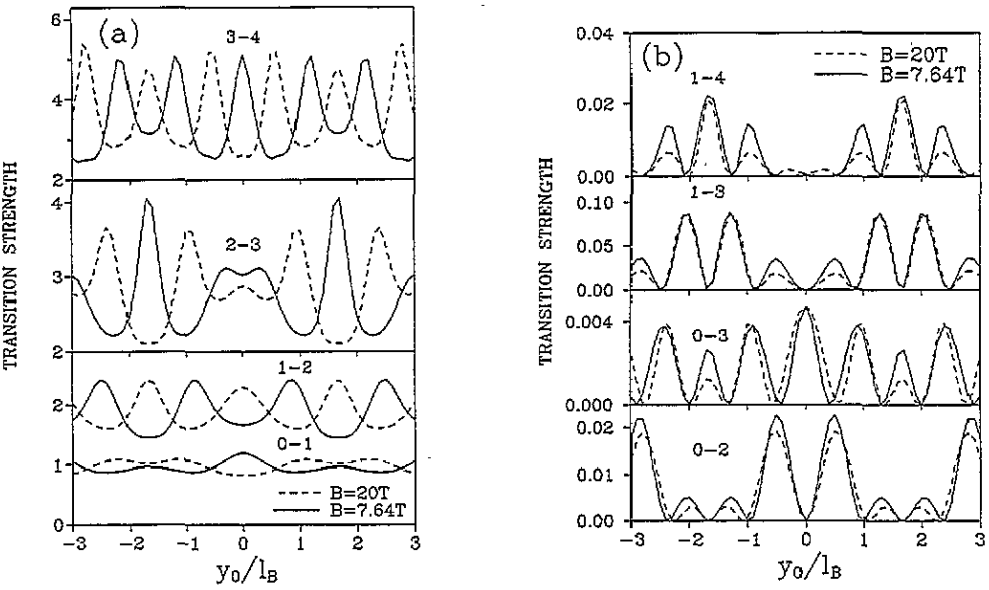

Figure 6. Same as in figure 5, for $B' = B\tau^2 = 7.64$ T (——) and $B'' = B\tau^4 = 20$ T (– – –).

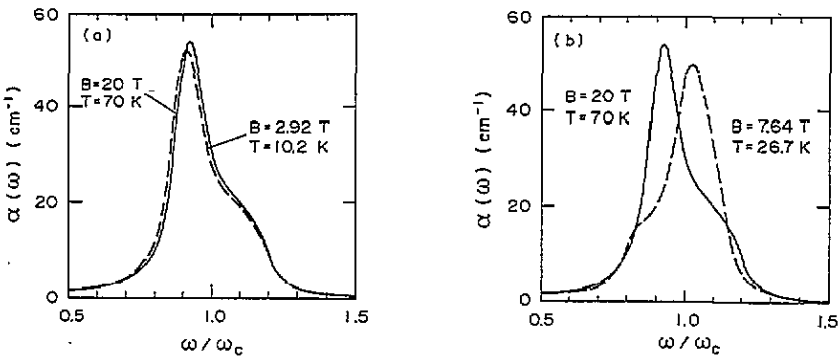

Figure 7. Intraband absorption coefficients $\alpha(\omega)$ for magnetic fields (a) $B = 2.92$ T and $B'' = B\tau^4 = 20$ T and (b) $B' = B\tau^2 = 7.64$ T and $B'' = B\tau^4 = 20$ T.

It is important to note that, for each of the magnetic fields considered above, the transition strengths (see figures 5 and 6) have properties similar to those found for the case of periodic SLs [11, 12]. In fact, the $n \to n+1$ transitions and the y_0/l_B-dependence of the corresponding transition strengths display clear irregular oscillatory behaviours around the $n+1$ bulk cyclotron-resonance values. Moreover, the largest (smallest) values of $T_{n,n+1}$ are reached for values of y_0/l_B close to those for which the n and $n+1$ magnetic subbands are nearest (farthest apart from) each other. As in the case of periodic SLs [12], these properties follow immediately from the sum rule given in equation (7). It is also clear that, whereas in the bulk case the selection rule $\Delta n = \pm 1$ is satisfied, the presence of the FSL potential makes it possible that intraband transitions with $\Delta n \neq \pm 1$ occur.

In order to illustrate the possibility of observing self-similarity (or anti-self-similarity) in a real experiment (such as an n-doped GaAs–(Ga, Al)As FSL [12]), we have calculated the scaled intraband absorption coefficients for $B = 2.92$ T, $B' = B\tau^2 = 7.64$ T and

$B'' = B\tau^4 = 20$ T (figure 7); note that the corresponding temperatures, energy-broadening parameters [12] and $\hbar\omega$ energies are scaled with $\hbar\omega_c$. It is clear then that, for magnetic fields scaled by τ^4, the intraband magneto-absorption spectra are self-similar whereas, for fields scaled by τ^2, the spectra are essentially anti-self-similar (one spectrum is approximately the mirror reflection of the other). It is also apparent that the most important contribution for the intraband absorption coefficient corresponds to transitions involving Landau levels $n = 0$ and $n = 1$ (cf figure 8, and figures 5 and 6). One may see that the intraband absorption spectra exhibit a sharp peak and a shoulder and may be characterized as an inhomogeneous broadened line. Note also that the structures in the $\alpha(\omega)$ absorption spectra correspond essentially to regions of absolute maxima and minima for $\Delta E = (E_1 - E_0)/\hbar\omega_c$ corresponding to transitions involving Landau levels $n = 0$ and $n = 1$ (cf figure 8).

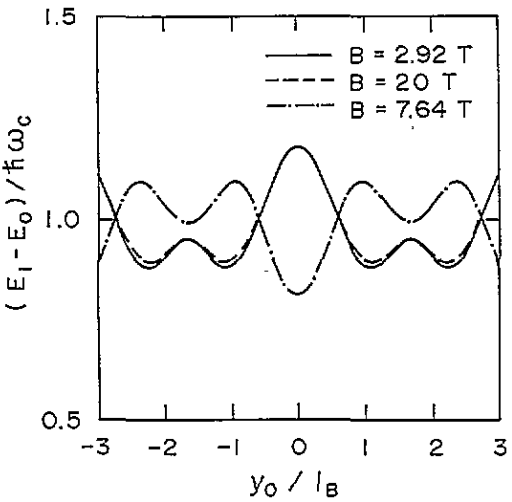

Figure 8. Energy differences between magnetic subbands corresponding to Landau levels $n = 0$ and $n = 1$ of a GaAs–(Ga, Al)As quasi-periodic FSL under in-plane magnetic fields of $B = 2.92$ T (——), $B' = B\tau^2 = 7.64$ T (— · —), and $B'' = B\tau^4 = 20$ T (– – –) as functions of the orbit-centre position. Energies and lengths are in units of the cyclotron energy and cyclotron radius, respectively.

5. Conclusions

We have presented a theoretical study of the magnetic subbands, electron wavefunctions, intraband transition strengths and intraband magneto-optical absorption coefficients in GaAs–(Ga, Al)As FSLs in the $B_\parallel$ configuration and Voigt geometry. Calculations were performed within the effective-mass approximation, with a parabolic model for the conduction band, and with envelope wavefunctions and magnetic subbands obtained by the method of expansion in harmonic-oscillator wavefunctions. Results were obtained for magnetic fields related by τ^2 and τ^4 with corresponding magnetic levels, electron wavefunctions, transition strengths and $\alpha(\omega)$ intraband absorption coefficients displaying either a self-similar or anti-self-similar behaviour as appropriate for a GaAs–(Ga, Al)As FSL.

It should be pointed out that theoretical calculations [11, 12] similar to those presented here were useful in understanding cyclotron-resonance experiments [14] (intraband optical absorption) performed on n-doped GaAs–(Ga, Al)As periodic SLs in the $B_\parallel$ configuration.

To our knowledge, up to now there have been no experiments on intraband transitions in GaAs–(Ga, Al)As FSLs. We do hope, however, that the theoretical results presented here will motivate such experiments and contribute to their understanding.

Acknowledgments

LEO is grateful to the hospitality of the Department of Theoretical Physics of the University of Havana, where this work was performed, and to the Brazilian Agencies CAPES, FINEP and CNPq for partial financial support.

Appendix

In this appendix, we demonstrate that a scaling of τ^{2n} in the magnetic field leads to self-similarity or anti-self-similarity in the energy-level structure and wavefunctions for a GaAs–(Ga, Al)As FSL, provided that the FSL potential could be substituted by its appropriate average value [7].

Let $\Psi_n(u-u_0)$ and $\Psi'_m(u-u_0)$ be the eigenfunctions of equation (8), for magnetic fields B and $B'' = B\tau^4$ (self-similar case), respectively. It is straightforward then to show that

$$\langle\Psi'_m(u-u_0)|v(u)-v'(u)|\Psi_n(u-u_0)\rangle = [E_n(u_0)-E'_m(u_0)]\langle\Psi'_m(u-u_0)|\Psi_n(u-u_0)\rangle. \tag{A1}$$

In the above expression, $E_n(u_0)$ and $v(u)$ ($E'_m(u_0)$ and $v'(u)$) are the corresponding energy and scaled FSL potential for the magnetic field B ($B'' = B\tau^4$).

If we now introduce the average (in the manner defined by Wang and Maan [7]) reduced potential $\bar{v}(u)$ of the FSL corresponding to the magnetic field B, then one obtains

$$\bar{v}(u) = v'(u) + \beta \tag{A2}$$

with $\beta = v_0/\tau^3$, and v_0 being the (Ga, Al)As barrier height in units of the cyclotron energy for the magnetic field B; now, if one considers that self-similarity occurs in the energy-level structure and wavefunctions (at least for small values of the Landau subband index), i.e. $E_n(u_0) \simeq E'_n(u_0)+\gamma$, and $\Psi'_n(u-u_0) \simeq \Psi_n(u-u_0)$, where γ is a constant, (A1) becomes

$$\langle\Psi_m(u-u_0)|v(u)-\bar{v}(u)|\Psi_n(u-u_0)\rangle \simeq (\gamma-\beta)\delta_{m,n}. \tag{A3}$$

The above equation implies that the matrix elements of both $v(u)$ and $\bar{v}(u)$ are essentially the same (provided that the energies of the B and $B'' = B\tau^4$ physical situations are displaced by $\gamma = \beta = v_0/\tau^3$). Therefore, if self-similarity occurs for the energy spectra and wavefunctions (corresponding to a given FSL in fields B and $B'' = B\tau^4$), one may replace the actual potential v (FSL in field B) by its average potential $\bar{v}$ when calculating matrix elements. On the other hand, if one substitutes v by $\bar{v}$, equation (A1) becomes

$$[E_n(u_0)-E'_m(u_0)-\beta]\langle\Psi'_m(u-u_0)|\Psi_n(u-u_0)\rangle = 0 \tag{A4}$$

and self-similarity for the energy spectra (displaced by $\beta = v_0/\tau^3$; this shift was indeed confirmed in the calculations as shown in figure 2(a)) and wavefunctions immediately follows.

Therefore, a necessary and sufficient condition for self-similarity in energy and wavefunctions (for magnetic fields B and $B'' = B\tau^4$) to occur is that the actual GaAs–(Ga, Al)As FSL potential (in a B magnetic field) could be replaced [7] by its average value. Of course, the above replacement and the conditions for which the above-mentioned

behaviour occurs break down for sufficiently high magnetic fields, high barriers, thick barriers and wells, and large values of the Landau subband index.

For a scaling in the magnetic field as in $B' = B\tau^2$, one may prove, in a similar way, that anti-self-similarity in the energy spectra and deviations of the wavefunctions (with respect to the $v = 0$ case) would follow.

References

[1] Esaki L and Tsu R 1970 *IBM J. Res. Dev.* **14** 61
See also Keldysh L V 1962 *Fiz. Tverd. Tela* **4** 2265 (Engl. Transl. 1963) *Sov. Phys. Solid State* **4** 1658

[2] Silin A P 1985 *Sov. Phys.–Usp.* **28** 972
Bastard G 1985 *J. Lumin.* **30** 488

[3] Sokoloff J B 1985 *Phys. Rep.* **126** 189

[4] MacDonald A H 1987 *Interfaces, Quantum Wells, and Superlattices* ed C R Leavens and R Taylor (New York: Plenum) p 347

[5] Merlin R, Bajema K, Clarke R, Juang F Y and Bhattacharya P K 1985 *Phys. Rev. Lett.* **55** 1768

[6] Laruelle F and Etienne B 1988 *Phys. Rev.* B **37** 4816

[7] Wang Y Y and Maan J C 1989 *Phys. Rev.* B **40** 1955

[8] Laruelle F, Paquet D, Joncour M C, Jusserand B, Barrau J, Mollot F and Etienne B 1990 *Localization and Confinement of Electrons in Semiconductors (Springer Series in Solid-State Science 97)* ed F Kuchar, H Heinrich and G Bauer (Berlin: Springer) p 258
Laruelle F, Etienne B, Barrau J, Khirouni K, Brabant J C, Amand T and Brousseau M 1990 *Surf. Sci.* **228** 92

[9] Munzar D, Bočáek L, Humlíček J and Ploog K 1994 *J. Phys.: Condens. Matter* **6** 4107

[10] Toet D, Potemski M, Wang Y Y, Maan J C, Tapfer L and Ploog K 1991 *Phys. Rev. Lett.* **66** 2128
Maan J C, Chitta V, Toet D, Potemski M and Ploog K 1992 *Springer Series in Solid-State Science* vol 101, ed G Landwehr (Berlin: Springer) p 549

[11] de Dios-Leyva M, Galindo V and Gondar J L 1992 *Phys. Rev.* B **45** 1923

[12] de Dios Leyva M and Galindo V 1993 *Phys. Rev.* B **48** 4516

[13] Kolář M and Ali M K 1989 *Phys. Rev.* B **39** 426

[14] Duffield T, Bhat R, Koza M, Hwang D M, DeRosa F, Grabbe P and Allen S J Jr 1988 *Solid State Commun.* **65** 1483 and references therein